2013 IEEE/RSJ International Conference on
Intelligent Robots and Systems (IROS)
November 3-7, 2013. Tokyo, Japan

Vibration Suppression Control of a Space Robot with Flexible Appendage based on Simple Dynamic Model*

Daichi Hirano[1], Yusuke Fujii[1], Satoko Abiko[2], Roberto Lampariello[3], Kenji Nagaoka[1] and Kazuya Yoshida[1]

Abstract— **This paper discusses a vibration suppression control method for a space robot with a rigid manipulator and flexible appendage. A suitable dynamic model that considers the coupling between the manipulator and flexible appendage was developed for the controller to accomplish the vibration suppression control of the flexible appendage. The flexible appendage was modeled using a virtual joint model, and the control method was developed on the basis of this model. Although this type of control requires feedback of the flexible appendage state, its direct measurement is generally difficult. Thus, an estimator of the flexible appendage state was constructed using a force/torque sensor attached between the base and flexible appendage. The control method was experimentally verified using an air-floating system.**

I. INTRODUCTION

Spacecraft with robot manipulators have been developed to capture space debris and repair space structures [1][2]. Most of these spacecraft need to be equipped with flexible appendages such as solar panels and antennas, as shown in Fig. 1. For a free-flying system in a micro-gravity environment, the reaction of the manipulator motion used for a given task excites a change in the base attitude, which induces vibrations in any other flexible appendages. These vibrations reduce the accuracy of operation, increase the risks of failure, cause wear-and-tear that shortens the life expectancy, and require a stronger and heavier mechanical design, which translates into higher costs. In order to suppress such vibrations during operation, an appropriate control method that considers the dynamic coupling among the manipulator, base, and flexible appendage is required.

There is a limited amount of research being conducted on the control of a space robot that considers the coupling between rigid manipulators and flexible appendages. In [3], the dynamics and control of such a system were studied. However, in their research, the equations of motion of the rigid manipulator and the flexible appendage were solved separately. This computation ignored dynamic coupling, which can lead to closed-loop instability [4].

*This research was partially supported by a Grant-in-Aid for JSPS Fellows (23-6651).

[1]D. Hirano, Y. Fujii, K. Nagaoka and K. Yoshida are with Department of Aerospace Engineering, Graduate School of Engineering, Tohoku University, 6-6-1 Aramaki, Aoba-ku, Sendai, 980-8579, Japan {hirano, y-fujii, nagaoka, yoshida} at astro.mech.tohoku.ac.jp

[2]S. Abiko is with Department of Mechanical Systems and Design, Graduate School of Engineering, Tohoku University, 6-6-1 Aramaki, Aoba-ku, Sendai, 980-8579, Japan abiko at space.mech.tohoku.ac.jp

[3]R. Lampariello is with the Institute of Robotics and Mechatronics, German Aerospace Center (DLR), Germany Roberto.Lampariello at dlr.de

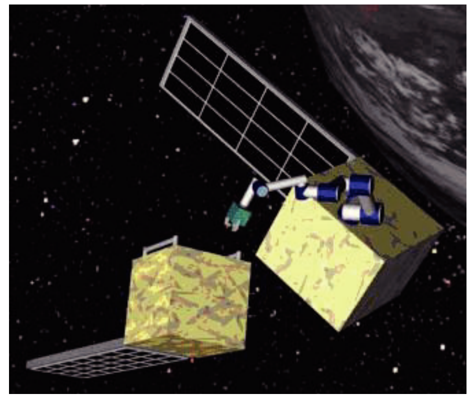

Fig. 1. Illustration of on-orbit servicing

The reactionless control of a manipulator was proposed by Nenchev [5]. This control method realizes manipulator motion that does not excite motion of the base by using the null-space of a redundant manipulator. However, the manipulator motion is severely restricted by the null-space limitations. Therefore, this method is not sufficient for tasks requiring manipulator motion over a large area.

Numerous studies in various fields have modeled and analyzed flexible arms or appendages [6][7]. The assumed mode method and finite element method are commonly used to analyze the behavior of a flexible appendage. The attitude control method for satellites with flexible panels employs the assumed mode method to model flexible panels [8][9]. To estimate the panel state, it requires several sensors such as piezoelectric elements on the panel or a visual monitoring system. In general, these devices make the system and operation more complex. The finite element method is impractical for online feedback control because of its high calculation cost. In contrast, Yoshikawa proposed a virtual joint model, which approximates flexible manipulators as virtual rigid links and passive spring joints [10]. This model expresses a complex flexible manipulator as a simple articulated body with dominant dynamic characteristics. We employed this model into a free-flying system. Using this method, a free-flying robot with flexible appendages can be modeled as a reduced articulated body system. This reduced model makes it possible to calculate the dynamics of the robot in real time using the limited computational resources of currently available hardware. Therefore, in this research, we developed the theory and technology which can be used in actual missions, using a virtual joint model.

In this study, we developed a simple dynamic model of a space robot with a rigid manipulator and flexible appendage,

978-1-4673-6357-0/13/$31.00 ©2013 IEEE

considering their coupling. Vibration suppression control and state estimator of the flexible appendage are proposed on the basis of this simple dynamic model. Their effectiveness was verified experimentally through the use of an air-floating system.

II. DYNAMIC MODEL

A. Dynamic Model of Flexible Appendage

A cantilever with a tip mass was considered as a flexible appendage, as shown in Fig. 2(a). We approximated the cantilever as a virtual joint model with one rigid link and one passive joint, as shown in Fig. 2(b). This virtual joint model has the stiffness of joint K_f as the unknown parameter. The method to identify the parameter is described below.

The cantilever was assumed to be a Euler-Bernoulli beam. From the Rayleigh law, the first eigenfrequency is described by

$$f_b = \frac{1}{2\pi}\sqrt{\frac{3EI}{l_f^3(m_t + \frac{33}{140}m_s)}} \tag{1}$$

where E, I, l_f, m_s, m_t are the Young's modulus, second moment of the area, length, mass of beam, and mass of the tip, respectively.

In contrast, the eigenfrequency of the virtual joint model is represented as follows:

$$f_j = \frac{1}{2\pi}\sqrt{\frac{K_f}{I_f}} \tag{2}$$

where I_f is the moment of inertia of the link. Note that I_f is a function of the length of link l_f.

The unknown parameter can be identified by comparing the above eigenfrequencies.

B. Dynamic Model of Free-Flying Robot

A simple dynamic model is introduced here with a manipulator and flexible appendage which is approximated by the virtual joint model. As an example, Fig. 3 shows a dynamic model with a three-joint manipulator and a one-joint flexible appendage. We assumed that the robot is in a micro-gravity environment; therefore, gravity does not apply. Given that no external force and moment are exerted on the end-effector and base, the equation of motion of this free-flying system can be represented as follows [11]:

$$\begin{bmatrix} \boldsymbol{H}_b & \boldsymbol{H}_{bm} & \boldsymbol{H}_{bf} \\ \boldsymbol{H}_{bm}^T & \boldsymbol{H}_m & \boldsymbol{H}_{mf} \\ \boldsymbol{H}_{bf}^T & \boldsymbol{H}_{mf}^T & \boldsymbol{H}_f \end{bmatrix} \begin{bmatrix} \ddot{\boldsymbol{x}}_b \\ \ddot{\boldsymbol{\phi}}_m \\ \ddot{\boldsymbol{\phi}}_f \end{bmatrix} + \begin{bmatrix} \boldsymbol{c}_b \\ \boldsymbol{c}_m \\ \boldsymbol{c}_f \end{bmatrix} = \begin{bmatrix} \boldsymbol{0} \\ \boldsymbol{\tau}_m \\ \boldsymbol{\tau}_f \end{bmatrix} \tag{3}$$

where the symbols are defined as follows.

- $\boldsymbol{H}_b$: Inertia matrix of base
- $\boldsymbol{H}_m$: Inertia matrix of manipulator
- $\boldsymbol{H}_f$: Inertia matrix of flexible appendage
- $\boldsymbol{H}_{bm}$: Coupling inertia matrix between base and manipulator
- $\boldsymbol{H}_{bf}$: Coupling inertia matrix between base and flexible appendage
- $\boldsymbol{H}_{mf}$: Coupling inertia matrix between manipulator and flexible appendage

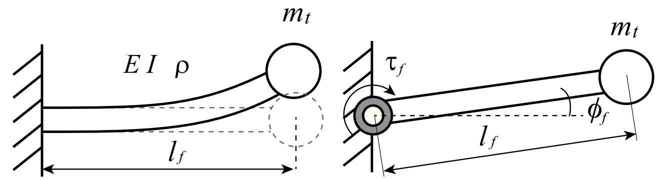

(a) Mass-cantilever model (b) Virtual joint model

Fig. 2. Models of flexible appendage

- $\boldsymbol{x}_b$: Vector of position and orientation of base
- $\boldsymbol{\phi}_m$: Vector of manipulator angle
- $\boldsymbol{\phi}_f$: Vector of flexible appendage angle
- $\boldsymbol{c}_b$: Nonlinear velocity-dependent term of base
- $\boldsymbol{c}_m$: Nonlinear velocity-dependent term of manipulator
- $\boldsymbol{c}_f$: Nonlinear velocity-dependent term of flexible appendage
- $\boldsymbol{\tau}_m$: Vector of torque on manipulator joints
- $\boldsymbol{\tau}_f$: Vector of torque on flexible appendage joints.

The torque of the flexible appendage is given by the following linearized form:

$$\boldsymbol{\tau}_f = -\boldsymbol{K}_f\boldsymbol{\phi}_f - \boldsymbol{D}_f\dot{\boldsymbol{\phi}}_f \tag{4}$$

where $\boldsymbol{K}_f$ and $\boldsymbol{D}_f$ are the matrices for the stiffness and damping, respectively, of the flexible appendage.

By eliminating the base acceleration term $\ddot{\boldsymbol{x}}_b$ from the middle and lower parts of (3) using the upper part of (3), the equation of motion can be rewritten in the following joint coordinate form [11]:

$$\hat{\boldsymbol{H}} \begin{bmatrix} \ddot{\boldsymbol{\phi}}_m \\ \ddot{\boldsymbol{\phi}}_f \end{bmatrix} + \hat{\boldsymbol{c}} = \begin{bmatrix} \boldsymbol{\tau}_m \\ \boldsymbol{\tau}_f \end{bmatrix} \tag{5}$$

where

$$\hat{\boldsymbol{H}} = \begin{bmatrix} \boldsymbol{H}_m & \boldsymbol{H}_{mf} \\ \boldsymbol{H}_{mf}^T & \boldsymbol{H}_f \end{bmatrix} - \boldsymbol{H}_{bc}^T\boldsymbol{H}_b^{-1}\boldsymbol{H}_{bc} \tag{6}$$

$$\hat{\boldsymbol{c}} = \begin{bmatrix} \boldsymbol{c}_m \\ \boldsymbol{c}_f \end{bmatrix} - \boldsymbol{H}_{bc}^T\boldsymbol{H}_b^{-1}\boldsymbol{c}_b \tag{7}$$

$$\boldsymbol{H}_{bc} = [\boldsymbol{H}_{bm} \;\; \boldsymbol{H}_{bf}]. \tag{8}$$

The matrix $\hat{\boldsymbol{H}}$ is referred to as the generalized inertia matrix.

III. CONTROL LAW

A control law is derived to suppress vibrations of the flexible appendage on the basis of the proposed model. The control inputs are the manipulator joints. The angular velocity of the flexible appendage is used for feedback to suppress the vibrations. The basic law of vibration suppression was introduced in [12]. The lower part of (5) can be expressed with the components of $\hat{\boldsymbol{H}}$ and $\hat{\boldsymbol{c}}$ as follows:

$$\hat{\boldsymbol{H}}_{fm}\ddot{\boldsymbol{\phi}}_m + \hat{\boldsymbol{H}}_f\ddot{\boldsymbol{\phi}}_f + \hat{\boldsymbol{c}}_f + \boldsymbol{D}_f\dot{\boldsymbol{\phi}}_f + \boldsymbol{K}_f\boldsymbol{\phi}_f = \boldsymbol{0} \tag{9}$$

where $\hat{\boldsymbol{H}}_f$ and $\hat{\boldsymbol{H}}_{fm}$ are components of the generalized inertia matrix for the flexible appendage and the coupling

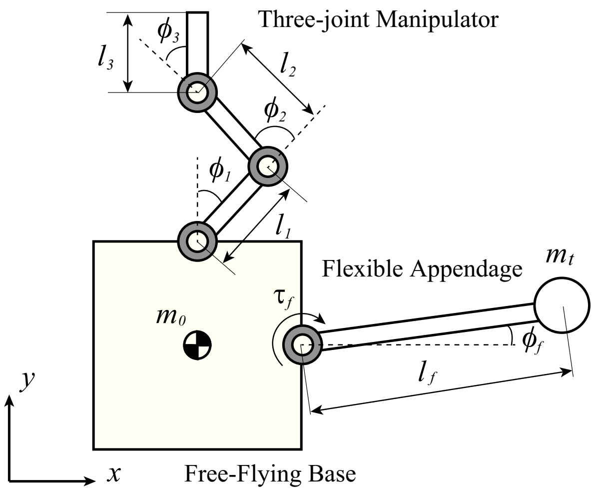

Fig. 3. Dynamic model of free-flying robot with flexible appendage

term between the manipulator and flexible appendage, respectively, and $\hat{\boldsymbol{c}}_f$ is a component of $\hat{\boldsymbol{c}}$ for the flexible appendage. By choosing a manipulator acceleration to satisfy

$$\hat{\boldsymbol{H}}_{fm}\ddot{\boldsymbol{\phi}}_m = \boldsymbol{D}_c\dot{\boldsymbol{\phi}}_f - \hat{\boldsymbol{c}}_f \tag{10}$$

where $\boldsymbol{D}_c$ is a control gain, the vibrations of the flexible appendage are suppressed according to the following equation of motion of a damping system.

$$\hat{\boldsymbol{H}}_f\ddot{\boldsymbol{\phi}}_f + (\boldsymbol{D}_c + \boldsymbol{D}_f)\dot{\boldsymbol{\phi}}_f + \boldsymbol{K}_f\boldsymbol{\phi}_f = \boldsymbol{0} \tag{11}$$

Note that the control gain $\boldsymbol{D}_c$ changes the damping ratio of the system. From the inverse solution of (10) , we obtain the desired angular acceleration of the manipulator in the following term:

$$\ddot{\boldsymbol{\phi}}_m^d = \hat{\boldsymbol{H}}_{fm}^+(\boldsymbol{D}_c\dot{\boldsymbol{\phi}}_f - \hat{\boldsymbol{c}}_f) \tag{12}$$

where the superscript "+" means the pseudo inverse. In practical use, the damping term of the manipulator is added as follows:

$$\ddot{\boldsymbol{\phi}}_m^d = \hat{\boldsymbol{H}}_{fm}^+(\boldsymbol{D}_c\dot{\boldsymbol{\phi}}_f - \hat{\boldsymbol{c}}_f) - \boldsymbol{D}_q\dot{\boldsymbol{\phi}}_m \tag{13}$$

where $\boldsymbol{D}_q$ stands for a damping matrix of the manipulator joints. Note that this control requires angular velocity feedback from the flexible appendage $\dot{\boldsymbol{\phi}}_f$. The state estimator of the flexible appendage for the feedback control is presented below.

IV. DESIGN OF STATE ESTIMATOR OF FLEXIBLE APPENDAGE

A. State Estimation

The state estimator of the flexible appendage for the feedback control is described here. In a case where the flexible appendage is modeled as a single virtual joint, the angular velocity of this virtual joint can be estimated using the force/torque sensor attached between the base and the flexible appendage.

Assuming that the damping term is small enough to vanish, the angle of the virtual joint can be represented from (4) as follows:

$$\boldsymbol{\phi}_f = \boldsymbol{K}_f^{-1}\boldsymbol{\tau}_f \tag{14}$$

where $\boldsymbol{\tau}_f$ is the torque measured by the force/torque sensor. The angular velocity $\dot{\boldsymbol{\phi}}_f$, which is used for the feedback control to suppress vibrations, can be obtained numerically from the differential value of $\boldsymbol{\phi}_f$ provided by (14) . However, the force/torque sensor often has zero offset. Although the angular velocity $\dot{\boldsymbol{\phi}}_f$ is not affected by this offset because it is obtained from the differentiation, the angle $\boldsymbol{\phi}_f$ is affected and difficult to measure with the force/torque sensor. Therefore, approximated inertia matrices that do not depend on the virtual joint angle are used to calculate the control input.

B. Approximation of Inertia Matrix

The vibration suppression control given by (13) requires the calculation of $\hat{\boldsymbol{H}}_{fm}$ and $\hat{\boldsymbol{c}}_f$, which are obtained from the inertia matrices $\boldsymbol{H}_b$ and $\boldsymbol{H}_{bc}$. These inertia matrices are the functions of the virtual joint angle $\boldsymbol{\phi}_f$. Because the direct measurement of the virtual joint angle is difficult as described above, we used the approximated inertia matrices. Suppose that the virtual joint angle of the flexible appendage is small and the inertia matrices can be approximated as the value around the equilibrium point: i.e.,

$$\boldsymbol{H}_b(\boldsymbol{\phi}_b, \boldsymbol{\phi}_m, \phi_f) \simeq \boldsymbol{H}_b(\boldsymbol{\phi}_b, \boldsymbol{\phi}_m, 0) \tag{15}$$

$$\boldsymbol{H}_{bc}(\boldsymbol{\phi}_b, \boldsymbol{\phi}_m, \phi_f) \simeq \boldsymbol{H}_{bc}(\boldsymbol{\phi}_b, \boldsymbol{\phi}_m, 0) \tag{16}$$

where $\boldsymbol{\phi}_b$ denotes the vector of the base attitude. From the above approximations, the inertia matrices become functions of measurable parameters.

V. EXPERIMENTAL STUDY

An experimental study was conducted to validate the proposed control based on the simplified model and estimated feedback value.

A. Experimental Setup

We developed an air-floating system to emulate a micro-gravity environment [13]. This system uses pressurized air to float a robot on a flat plane without friction and realize motion under the micro-gravity environment in two dimensions. Fig. 4 shows an air-floating robot with a three-joint manipulator and flexible appendage. The details of the model parameters are listed in Table.I. The symbols in this list are the same as shown in Fig. 3. This robot has a gyro on its base, which can measure its rotational angle and angular velocity. The manipulator can be controlled by joint velocity control. The manipulator encoders measure the angles of each joint and provide the angular velocities from its differential values. The flexible appendage is a cantilever with a tip mass. The measured values from the gyro on the base and the manipulator encoders are used for the feedback control. The dynamic calculation and input-output data transfer for the control are performed by an on-board computer.

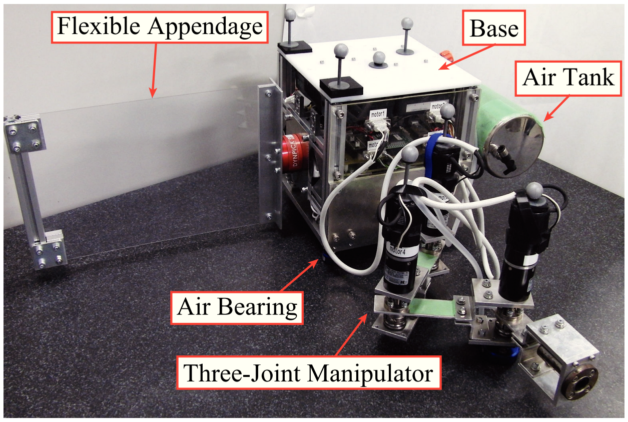

Fig. 4. Overview of air-floating robot

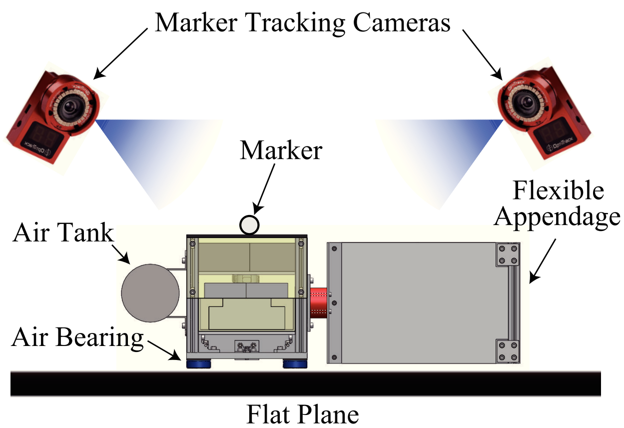

Fig. 5. Experimental setup

The motion of the robot and flexible appendage were measured using an external camera that tracked markers on the robot and flexible appendage, as shown in Fig. 5.

B. Experimental Conditions

In this experiment, we compared the results *with* and *without* the vibration suppression control.

The initial state of the robot was stable, and the configuration of the manipulator was a straight line(Fig. 6 (left)). During the experiment, the desired joint velocity was given as follows:

$$\dot{\phi}_m^d = \begin{cases} [-60 \;\; 120 \;\; -60]^T & [\text{deg/s}] \quad (0 \leq t < 1) \\ [0 \;\;\; 0 \;\;\; 0]^T & [\text{deg/s}] \quad (1 \leq t < 2) \\ \dot{\phi}_m + \ddot{\phi}_m^d \Delta t & \quad (2 \leq t) \end{cases} \tag{17}$$

where t denotes the experimental time and Δt stands for the time of the control loop. In this experiment, the control loop was set to 5 ms. In the first 1 s, the manipulator was controlled at a constant angular velocity. Vibrations in the flexible appendage were induced by this manipulator motion. During the period from 1 s to 2 s, the motion of the manipulator was stopped (Fig. 6 (middle)). At $t = 2$, the vibration suppression control began. The input was given to realize the desired angular acceleration in (13) according to the last term of (17) . The control gains were set to $D_c = 0.2$ and $D_q = 1.0$. The feedback value $\dot{\phi}_f$ was obtained by the state estimator. A block diagram of the control is shown in Fig. 7.

TABLE I

MODEL PARAMETER VALUES

l_1, l_2	0.120	[m]
l_3	0.067	[m]
l_f	0.210	[m]
m_0	8.590	[kg]
m_1	0.555	[kg]
m_2	0.621	[kg]
m_3	0.267	[kg]
m_t	0.320	[kg]
K_f	0.5561	[Nm/rad]
D_f	0.0013	[Nms/rad]

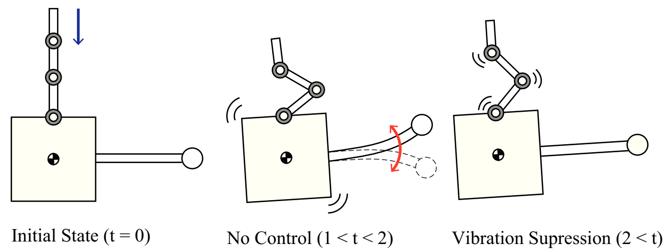

Fig. 6. Overview of robot motion

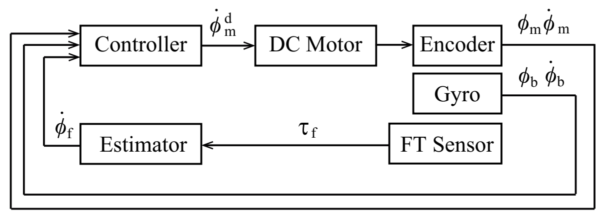

Fig. 7. Block diagram of control

C. Experimental Results

Figs. 8-13 show the experimental results for manipulator joint angles, tip deflections of the flexible appendage, panel angles, panel angular velocities, base positions, and base attitudes. The solid lines indicate the results *with* the control, and the dotted lines represent the results *without* the control. The time history of the manipulator joint angles is shown in Fig. 8. In the first 2 s, the manipulator motions in each case were the same. After that, the manipulator was activated to suppress the vibration in the vibration suppression control. The tip deflections of the flexible appendage are compared in Fig. 9. The vibration of the flexible appendage was suppressed by the manipulator motion. Figs. 10 and 11 show the results of angle and angular velocity of the virtual joint. In Fig. 11, the estimated angular velocity of the virtual joint with the control is presented as a red line. Compared to the actual value, the estimated value was delayed for 10 ms approximately due to filtering noise of the sensors. However,

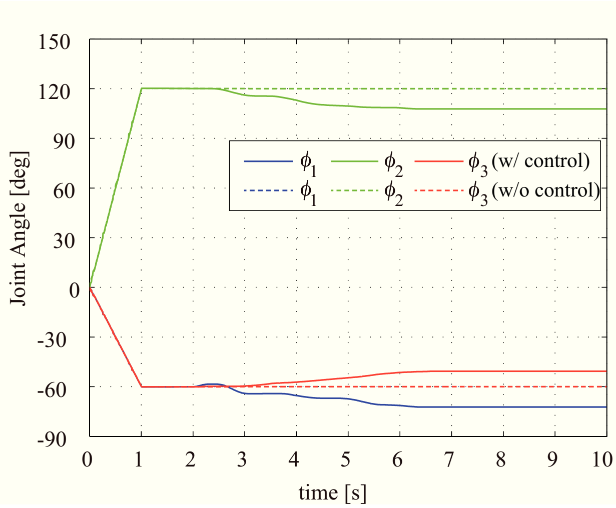

Fig. 8. Response of manipulator joint angles

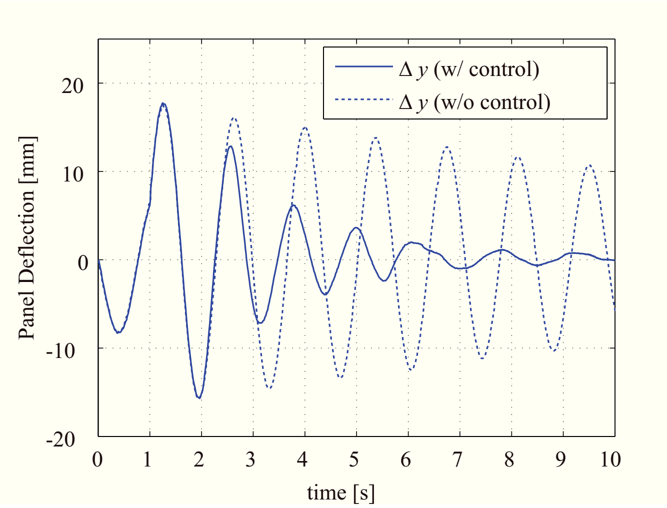

Fig. 9. Response of tip deflection of flexible appendage

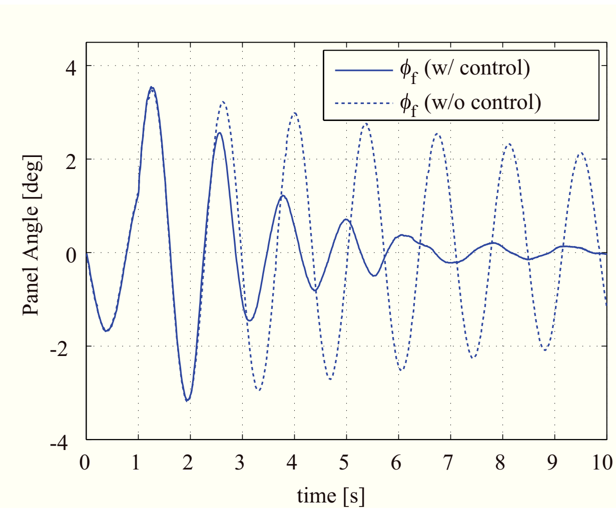

Fig. 10. Response of panel angle

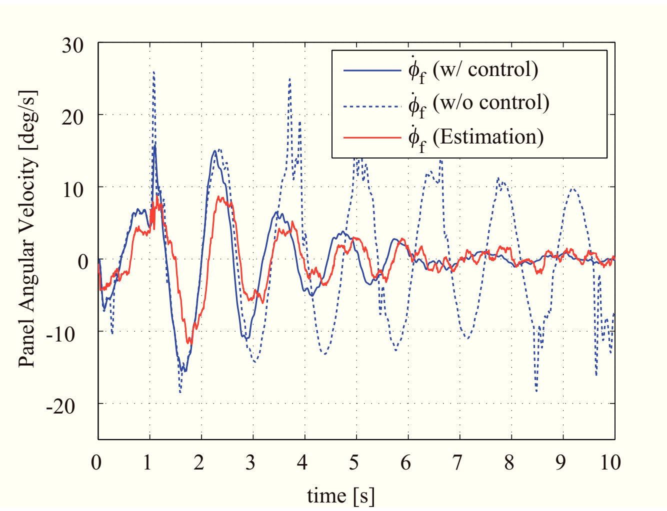

Fig. 11. Response of panel angular velocity

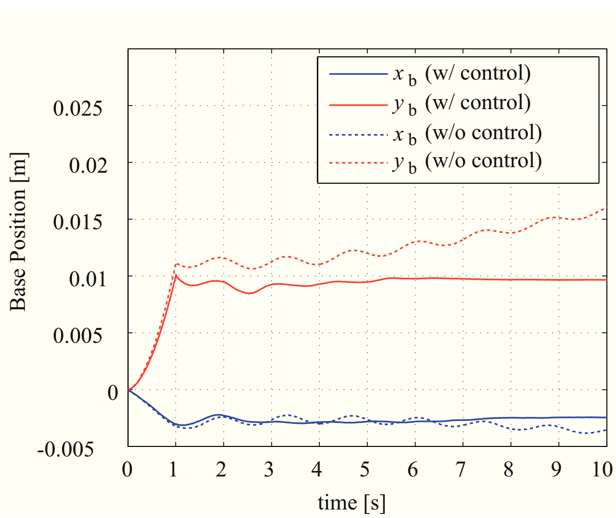

Fig. 12. Response of base position

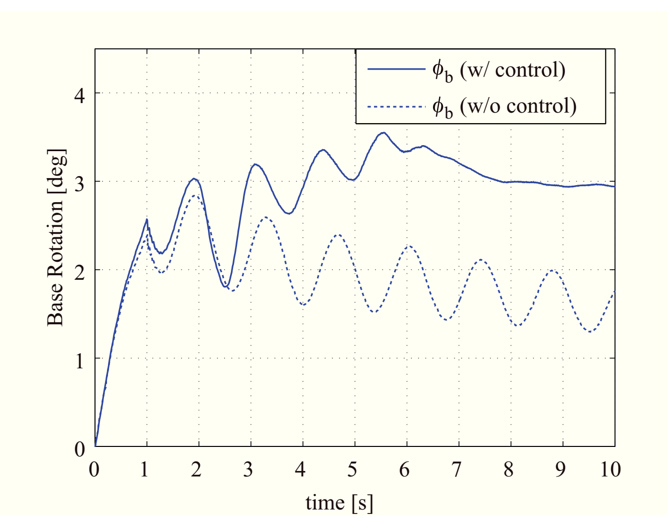

Fig. 13. Response of base attitude rotation

this time delay is sufficiently small in a comparison with the vibration period of the flexible appendage, and therefore the vibration suppression control can be realized. In Fig. 10, the vibration was suppressed successfully. The above results confirmed that the proposed vibration suppression control is effective for this system. As a result of the vibration suppression of the flexible appendage, as shown in Figs. 12 and 13, the vibrations of the base position and base attitude were also suppressed. In contrast, without the control, the base position and attitude continued to vibrate because the base was affected by the flexible appendage's vibration.

In Figs. 9 and 10, vibrations with a smaller amplitude were observed, while the dominant vibration with a higher amplitude was successfully suppressed. This may be due to the limitations of the sensor and actuator of the manipulator. The small deflections can not be measured exactly because of mechanical noise, and motion with a small angular velocity is difficult to realize because of the hardware limitations.

The above experimental results proved that the proposed simple model and control method using the state estimation for a flexible appendage are sufficiently able to suppress vibrations of a flexible appendage for a free-flying robot.

VI. CONCLUSIONS

We presented a feedback control method for suppressing the vibrations of a flexible appendage of a space robot. We proposed a simplified dynamic model and the state estimator of a flexible appendage that consider the coupling between a rigid manipulator and flexible appendage. A verification experiment demonstrated the practical viability of a feedback control method based on the proposed model and state estimation. The experimental results revealed their effectiveness.

In future work, we will investigate the theoretical stability of the proposed method for a case involving high amplitudes of higher vibrational modes. In addition, we intend to develop a control method to accomplish an end-effector motion and a vibration suppression simultaneously using manipulator redundancy.

REFERENCES

[1] F. Sellmaier, T. Boge, J. Spurmann, S. Gully, T. Rupp and F. Huber, On-orbit servicing mission: challenges and solutions for spacecraft operations, in Proc. SpaceOps 2010 Conf., Alabama, USA, AIAA No.2010-2159.

[2] F. Aghili, Optimal control of a space manipulator for detumbling of a target satellite, in Proc. 2009 IEEE Int. Conf. on Robotics and Automation (ICRA), Kobe, Japan, 2009, pp. 3019-3024.

[3] P. Zarafshan and S. A. A. Moosavian, Manipulation control of a space robot with flexible solar panel, in Proc. 2010 IEEE/ASME Int. Conf. on Advanced Intelligent Mechatronics, Montreal, Canada, 2010, pp. 1099-1104.

[4] J. L. Junkins and Y. Kim, Introduction to dynamics and control of flexible structure, AIAA Inc.,1993, pp. 140.

[5] D. N. Nenchev, K. Yoshida and M. Uchiyama, Reaction null-space based control of flexible structure mounted manipulator system, in Proc. 35th Conf. on Decision and Control, Kobe, Japan, 1996, pp. 4118-4123.

[6] M. Benosman and G. L. Vey, Control of flexible manipulators: A survey, Robotica, Vol. 22, 2004, pp. 533-545.

[7] S. K. Dwivedy and P. Eberhard, Dynamic analysis of flexible manipulators, a literature review, Mechanism and Machine Theory, Vol. 41, 2006, pp. 749-777.

[8] M. Shahravi and M. Kabganian, Attitude tracking and vibration suppression of flexible spacecraft using implicit adaptive control Law, in Proc. American Control Conference, Oregon, USA, 2005, pp. 913-918, vol. 2.

[9] D. Izzo and L. Pettazzi, Command shaping for a flexible satellite platform controlled by advanced fly-wheels systems, in Proc. 56th International Astronautical Congress, Fukuoka, Japan, 2005, 05-C.1.03.

[10] T. Yoshikawa and K. Hosoda, Modeling of flexible manipulators using virtual rigid links and passive joints, in Proc. 1991 IEEE/RSJ Int. Conf. on Intelligent Robotics and Systems (IROS), Osaka, Japan, 1991, pp. 967-972.

[11] Y. Xu and T. Kanade, Space robotics: dynamics and control, Kluwer, Dordrecht, 1993.

[12] K. Yoshida, D. N. Nenchev and M. Uchiyama, Vibration suppression and zero reaction maneuvers of flexible space structure mounted manipulators, Smart Materials and Structure, Vol. 8, No .6, 1999, pp. 847-856.

[13] N. Uyama, H. Lund, K. Asakimori, Y. Ikeda, D. Hirano, H. Nakanishi and K. Yoshida, Integrated experimental environment for orbital robotic systems using ground-based and free-floating manipulators, in Proc. 2010 IEEE/SICE Int. Symposium on System Integration, Kyoto, Japan, pp.108-113.